10.1109/ULTSYM.2014.0640

Designing Efficient CMUT Cells for Airborne Applications

Asli Unlugedik [a,b], A. Sinan Tasdelen [b], Abdullah Atalar [b] and Hayrettin Köymen [b]
[a] Dept. of Electrical Engineering, Stanford University, Stanford, CA 94305-9505,
[b] Dept. of Electrical and Electronics Engineering, Bilkent University, Ankara, Turkey 06800
Email: asli@ee.bilkent.edu.tr

***Abstract*—In this work, we study airborne CMUT cells with vacuum gap where silicon plate is operated both in elastically linear and nonlinear regimes. We report the results of a new mode of operation where the plate center swings the entire gap. The plate is kept in elastically linear region in this mode. Very large pressure levels are obtained at relatively low drive voltage levels. The operation is very efficient but the bandwidth is less than 1%. We considered operating the silicon membrane in elastically nonlinear region for larger bandwidth without sacrificing efficiency. This is achieved by employing the stiffening effect due to the atmospheric pressure. We derived the new model of the CMUT, where the membrane profile deviates from linear profile as a function of the differential static pressure on it. We present the force, the compliance models and the static analysis of stiffened CMUT cells in this work.**

Keywords-airborne CMUT; nonlinearity

I. INTRODUCTION

A cross sectional view of a circular airborne CMUT is shown in Fig. 1, where a is the diameter of the CMUT, t_{ge} is the effective gap height, t_i is the insulating layer thickness, t_m is the membrane thickness, and F is the total force exerted on the membrane. Acoustic wave is generated by applying an electrical signal between the electrodes of CMUT.

The mass of the plate must be kept at a minimum for a given operating frequency to achieve a wide bandwidth [1], since the radiation resistance of air is very low. However, CMUTs with thin radiating plates experience increased atmospheric pressure and therefore a larger static plate deflection. This causes nonlinearity in compliance and the plate becomes stiffer. This effect causes an increase in the resonance frequency of the CMUT. The resonance frequency is also affected by the nonlinearity in the transduction force, which has an opposite effect.

In the first part of this work, we propose a mode of operation where these two effects are counter balanced to provide a very large swing amplitude at resonance, while the deflection-to-membrane-thickness ratio is kept below 0.2. In this minimum voltage mode (MVM), the membrane center swings the entire gap at the lowest possible drive level in unbiased operation. In unbiased operation CMUT is driven with sinusoidal signal with zero bias voltage

$$V_{in} = V_m \cos\left(\frac{\omega}{2}t + \theta\right) \tag{1}$$

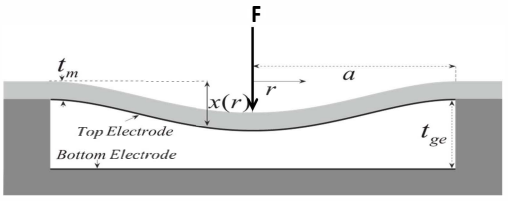

Fig.1. Cross sectional view of circular airborne CMUT.

An accurate circuit model-based characterization, given in [2], is used to make performance analysis [3]. The performances of the fabricated CMUTs are tested and compared with the circuit model results.

Airborne CMUTs are typically analyzed and designed to operate in elastically linear region. The linear regime constraint defines a limit on the achievable lowest quality factor and therefore on the widest achievable bandwidth. The limitation of the quality factor can only be overcome by using lighter and/or stiffer materials [4] as the membrane material.

In the second part of this paper, we present an approach to overcome this limitation and analyze airborne CMUTs in nonlinear regime to obtain a wider operation frequency band. It is shown that a wide bandwidth can be achieved by using silicon as a stiffened plate material. We present the transduction force, the compliance and the static analysis of CMUT cells with stiffened plates in nonlinear operation.

II. LINEAR REGION

The mechanical quality factor, Q_m, of a single CMUT cell operating in the linear region [1], is given by

$$Q_m = \frac{\omega_r L_{Rm} + X_{RR}(k_r a)}{R_{RR}(k_r a)} = \frac{k_r a}{R_1(k_r a)} \frac{t_m}{a} \frac{\rho_m}{\rho_0} + \frac{X_1(k_r a)}{R_1(k_r a)} \tag{2}$$

where k_r is the wave number in air at the resonance frequency R_1 and X_1 are the normalized radiation resistance and reactance of the CMUT cell and ρ_m/ρ_0 is the ratio of the density of plate material to that of air. Unfortunately, ρ_m/ρ_0 is very high for typical micromachining materials. The only means of having a lower quality factor in lossless CMUT is to have a very small t_m/a ratio. However, in a CMUT with vacuum gap, atmospheric ambient pressure deflects thinner plates, causing increased plate stiffness due to nonlinear effects [4]. Operation of a CMUT cell with a thin plate under

uniform pressure can be described using a linear mechanical model, if the center deflection (X_P) is less than one fifth of the plate thickness (t_m) [4].

The maximum displacement of the plate center is limited to gap height, which can be taken as t_{ge}, approximately.

$$\frac{t_{ge}}{t_m} = \frac{1}{(k_r a)^4 c_0^4 \rho_m^2} \frac{400}{27} \frac{Y_0 P_0}{(1-\sigma^2)} \left(\frac{F_{Pb}}{F_{Pg}}\right)^{-1} < 0.2 \qquad (3)$$

and the relation between t_m/a, and $k_r a$ can be obtained at the unstiffened mechanical resonance frequency as

$$\frac{t_m}{a} = (k_r a) c_0 \sqrt{\frac{9}{80} \frac{(1-\sigma^2)\rho_m}{Y_0}}. \qquad (4)$$

Fig. 2 and 3 can be used to design a CMUT cell with desired properties. F_{pb}/F_{pg}(<1) basically defines the fractional deflection of the plate under ambient pressure. With no applied bias voltage, it is equal to X_P/t_{ge}. Since the maximum deflection can be t_{ge}, for operation in linear regime, t_{ge}/t_m must be less than 0.2. Since a small $k_r a$ is desirable, it is best to choose F_{pb}/F_{pg} as large as possible. Having chosen the F_{pb}/F_{pg} and $k_r a$ values, t_{ge}/t_m and V_c/t_{ge} can be determined from Fig.2. Then, Fig. 3 can be used to find the values of Q_m and a/t_m.

Nearly optimal and practical values are obtained, when we choose F_{pb}/F_{pg}=0.8, $k_r a$=2.1 and use Fig.2 to get t_{ge}/t_m=0.194 and V_c/t_{ge}=14.6 V/µm. Fig. 3 gives Q_m=147 and a/t_m=33.3. Harmonic balance simulations show that a maximum swing (1- F_{pb}/F_{pg}) t_{ge}=0.2t_{ge} is obtained with an unbiased sinusoidal drive signal at a frequency of 0.497f_r with a 0.188V_c peak amplitude.

For example, at f_r=100 kHz (k_r=1848), we find a=1.14 mm. Hence t_m=34.2 µm, t_{ge}=6.64 µm and V_c=96.7 V. We find the maximum peak swing amplitude (1–F_{pb}/F_{pg})t_{ge}=1.32 µm. This swing amplitude is reached using an unbiased sinusoidal input signal at 49.7 kHz, with 18.2 V peak value.

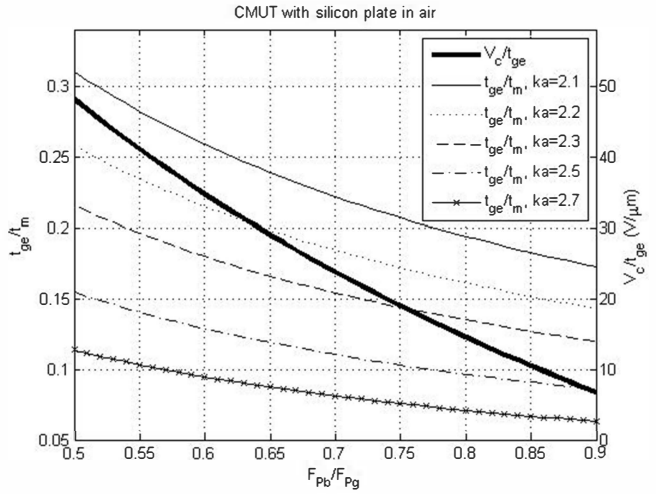

Fig. 2. Design graph for a CMUT with silicon plate operating in air. V_c is the collapse voltage under ambient pressure.

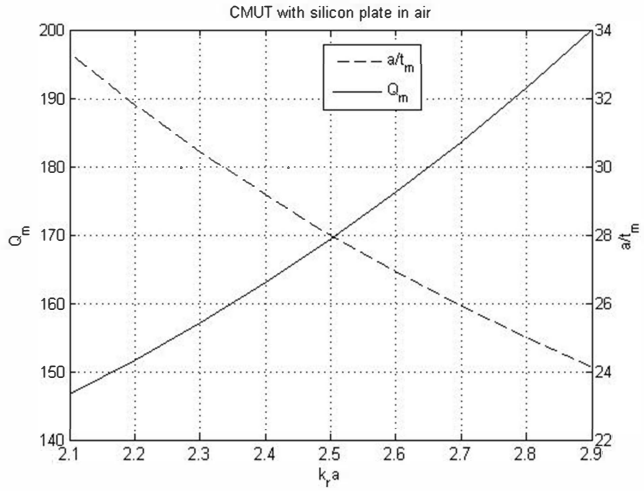

Fig. 3. Design graph for a CMUT with silicon plate operating in air.

It is analytically proven that possible lowest quality factor in mechanically linear region for a lossless silicon plate is 140 [3]. The quality factor can be decreased by introducing loss mechanism which decreases the efficiency. Operating the CMUT in elastically nonlinear region provides larger bandwidth without sacrificing efficiency.

III. CMUT WITH STIFFENED PLATE

The only way to achieve low loss and low quality factor simultaneously is to increase radius to plate thickness ratio, a/t_m, [1]. As a/t_m is increased the plate becomes more compliant. The center deflection-to-thickness ratio may exceed 0.2 due to the atmospheric pressure. The stiffness of the plate increases and the resonance frequency shifts upwards. As a result, a relatively thin plate may act like a high stiffness material when it is deflected beyond its linear operation limits.

A. *Profile of Stiffened Plate*

The displacement profile assumed in [2] is not applicable for stiffened plate. A very good approximation to stiffened profile is obtained using the following profile

$$x(r) \approx X_P \frac{\left(1-\frac{r^2}{a^2}\right)^2}{\left(1-\gamma\frac{r^2}{a^2}\right)} \qquad (5)$$

where X_P is the center deflection and

$$\gamma \approx 1 - \frac{1}{1+0.2938(w)^2 - 1.123\times10^{-3}(w)^4 + 2.657\times10^{-6}(w)^6} \qquad (6)$$

Here, $w = X_P/t_m$ is the deflection to membrane thickness ratio.

The *average* and *rms* displacements for the profile in (5) differ from [2] and are as follows:

The average displacement, X_A, is defined as

$$\frac{X_{Av}}{X_P} = 2\int_0^1 \frac{\left(1-\rho^2\right)^2}{\left(1-\gamma\rho^2\right)}\rho d\rho = A(w) \tag{7}$$

where

$$A(w) \approx \frac{1}{3}\frac{1}{0.67005 + 1/\nu_A}, \tag{8}$$

with

$$\nu_A = 0.00094(w)^4 - 0.03725(w)^3 + 0.68772(w)^2 + 3.030762 \tag{9}$$

and the rms displacement, X_R, is defined as

$$\frac{X_R}{X_P} = \sqrt{2\int_0^1 \left[\frac{\left(1-\rho^2\right)^2}{\left(1-\gamma\rho^2\right)}\right]^2 \rho d\rho} = B(w) \tag{10}$$

where

$$B(w) \approx \frac{1}{\sqrt{5}}\frac{1}{0.782105 + 1/\nu_B}, \tag{11}$$

$$\nu_B = 0.0043(w)^4 - 0.04065(w)^3 + 1.04479(w)^2 + 4.589366 \tag{12}$$

B. Induced stress

The induced stress at the rim of a thin silicon membrane is studied by finite-element-analysis (FEA) [1], where it is found to be proportional to the square of t_m/a ratio and its dependence on X_P/t_m is also reported. The induced maximum stress, T_{im}, can be accurately modeled as

$$T_{im} \approx \frac{16\pi Y_0}{\left(1-\sigma^2\right)}\left(\frac{t_m}{a}\right)^2\left[0.10926(w)^2 + 0.03445(w)\right] \tag{13}$$

where Y_0 is the Young's modulus and σ is the Poisson ratio of silicon. Hence, for an allowable maximum induced stress, T_{max}, we must have

$$\frac{a}{t_m} > 0.338(w)\sqrt{\frac{16\pi Y_0}{\left(1-\sigma^2\right)}\frac{1}{T_{im}}}. \tag{14}$$

For example, if a safe maximum allowable stress in silicon is T_{im}=500 MPa, then

$$\frac{a}{t_m} > 42w \tag{15}$$

for large w. Therefore, to allow a plate center deflection of twice its thickness (w=2), the radius must be larger than 1.26 mm for a 15 µm thick silicon membrane.

C. Energy

The potential energy in the membrane is calculated as

$$E_P = E_{Pm} + \frac{2\pi\varepsilon_0}{2}V^2\int_0^a \frac{rdr}{t_{ge} - x(r)} \left\{ = \frac{\pi a^2\varepsilon_0}{X_P}V^2\int_0^1 \frac{\rho d\rho}{\frac{t_{ge}}{X_P} - \frac{x(\rho)}{X_P}} \right\} \tag{16}$$

where E_{Pm} is potential energy due to static pressure.

$$E_P = E_{Pm} + \frac{C_0V^2}{2}g_s(\gamma,u) \tag{17}$$

where $u = X_P/t_{ge}$, is the deflection normalized to effective gap height, and

$$g_s(\gamma,u) = \frac{1}{\frac{X_P}{t_{ge}}}\left\{\left(\frac{\gamma^2 + 2(1-\gamma)u}{\sqrt{\gamma^2 + 4(1-\gamma)u}}\right) \arctanh\left(\frac{\sqrt{\gamma^2 + 4(1-\gamma)u}}{(2-\gamma)}\right) + \frac{\gamma}{2}\ln\left(\frac{1-\gamma}{1-u}\right)\right\} \tag{18}$$

D. Transduction Force

Transduction force is obtained by evaluating the gradient of the energy along X_R:

$$f_R = \frac{d\left(E_{pe}\right)}{dX_R} = \frac{1}{B(w) + \frac{X_P}{t_m}\frac{d}{dw}B(w)}f_P \tag{19}$$

where

$$f_P = \frac{d\left(E_{Pe}\right)}{dX_P} = \frac{C_0V^2}{2t_{ge}}\left[\frac{dg_s}{du} + \frac{dg_s}{d\gamma}\frac{d\gamma}{du}\right] = \frac{C_0V^2}{2t_{ge}}g_s' \tag{20}$$

E. Compliance

Nonlinear dependence of the compliance on the deflection of the plate is studied in [1], where an FEA-based method to quantify this dependence is also given. A very good approximation to this variation can be expressed as:

$$\frac{C_R}{C_{Rm}} \approx \frac{1}{1 + 0.61712(w)^2 - 0.00698(w)^3} = \frac{1}{p_C\left(t_{ge}/t_m\right)} \tag{21}$$

where, C_{Rm}, *rms* compliance in linear equivalent circuit model is given in [2].

F. Static Ambient pressure

For the displacement profile given by (2) the *rms* static ambient pressure differs from [2] and it is defined as

$$F_{bR} = \frac{A_f(w)}{B_f(w)} \pi a^2 P_0 \tag{22}$$

where

$$A_f(w) = A(w) + w\frac{d}{dw}A(w) \tag{23}$$

and

$$B_f(w) = B(w) + w\frac{d}{dw}B(w) \tag{24}$$

IV. Static Analysis

The static force equilibrium between transduction force, force due to ambient pressure and restoring force is given as

$$F_R + F_{Rb} = \frac{X_R}{C_{Rm}} \tag{25}$$

This equilibrium can be expressed as

$$\frac{V_{DC}}{V_r} = \sqrt{\frac{3}{2}\frac{5B_f(w)B(w)p_C(t_{ge}/t_m)u - 3A_f(w)\frac{F_b}{F_g}}{g_s'(t_{ge}/t_m, u)}} \tag{26}$$

as in [2], where V_r is the collapse voltage for an unstiffened CMUT in vacuum and F_g is the force required to deflect the membrane center by t_{ge}.

CMUT biasing chart (CBC) [2] for stiffened membrane is depicted in Fig. 4 using (23). The collapse voltage for a given normalized deflection and static bias increases as the membrane is stiffened. The depression due to static pressure is no longer equal to F_b/F_g as in unstiffened CMUT [2], but it is a function of t_{ge}/t_m and F_b/F_g. The collapse line is also shown in the Fig 4.

The collapse voltage of the CMUT also increases as the membrane is stiffened. The collapse voltage of stiffened membrane in vacuum is a function of t_{ge}/t_m, $V_{rs}(t_{ge}/t_m)$. The collapse lines for different t_{ge}/t_m values and $V_{rs}(t_{ge}/t_m)$ are depicted in Fig. 5.

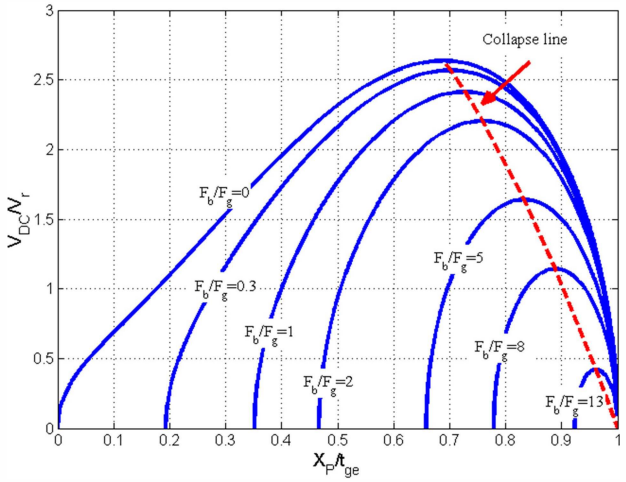

Fig.4. CBC of CMUT with stiffened membrane for t_{ge}/t_m=5.

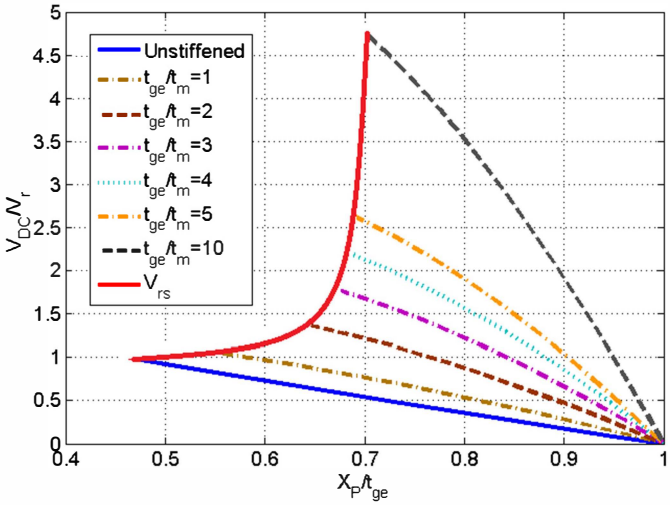

Fig.5. $V_{rs}(t_{ge}/t_m)$ and collapse lines for CMUTs with t_{ge}/t_m varying from unstiffened to 10.

Acknowledgement

This work is supported in part by Turkish Scientific and Research Council (TUBITAK) under project grants 110E216. AA thanks TUBA for the research support.

References

[1] A. Unlugedik, A. Atalar, and H. Koymen, "Designing an efficient wide bandwidth single cell CMUT for airborne applications using nonlinear effects," in *Proc. IEEE Ultrasonics Symp.*, 2013, pp.1416–1419.

[2] H. Koymen, et al., "An improved lumped element nonlinear circuit model for a circular CMUT cell," IEEE Trans. on Ultrason., Ferroelec. and Freq. Cont., vol. 59, no. 8, pp. 1791–1799, August 2012.

[3] A.Unlugedik, *et al.*, "Designing transmitting CMUT cells for airborne applications," IEEE Trans. on Ultrason., Ferroelec. and Freq. Cont., accepted.

[4] A.M. Cetin, and B. Bayram, "Diamond-based capacitive micromachined ultrasonic transducers in immersion,"IEEE Trans. Ultrason. Ferroelect. Freq. Contr., vol. 60, pp.414-420, 2013.

[5] E. Ventsel and T. Krauthammer, *Thin plates and shells*, 1st ed., New York: Marcel Dekker Inc., 2001.

[6] M. Kupnik, I. O. Wygant, and Butrus T. Khuri-Yakub, "Finite element analysis of stress stiffening effects in CMUTs," in *Proc. IEEE Ultrasonics Symp.*, 2008, pp. 487–490.